

Active species in Ar-O₂ and Ar-O₂-N₂ flowing microwave discharges and post-discharges

Kinga Kutasi¹, Vasco Guerra², Paulo Sá^{2,3}, Jorge Loureiro²

¹Research Institute for Solid State Physics and Optics of the Hungarian Academy of Sciences, POB 49, H-1525 Budapest, Hungary

²Instituto de Plasmas e Fusão Nuclear, Instituto Superior Técnico, 1049-001 Lisboa, Portugal

³Departamento de Engenharia Física, Faculdade de Engenharia da Universidade do Porto, 4200-465 Porto, Portugal

Abstract: This work presents a theoretical investigation on the production of active species in low-pressure Ar-O₂ and Ar-O₂-N₂ microwave discharges. Special attention is given to the species relevant for plasma sterilization, such as Ar(4s) excited states, O(³P) and O(¹D) atoms, NO(A) and NO(B) molecules. It is shown that, for the conditions of the present study, the active species are efficiently produced in the discharge and can be transported to a reaction chamber, as long as the early-afterglow time does not exceed $\sim 10^{-4}$ s.

Keywords: kinetic modeling, hydrodynamic modeling, surface wave discharge, afterglow

1. Introduction

Ar-O₂ plasmas are widely used in material processing and biomedical applications, e.g. the post-discharge of Ar-O₂ has been successfully used as oxidizing media in deposition of oxide films [1], and the inactivation of bacterial spores have been achieved in the flowing afterglow of an Ar-O₂ microwave discharge [2]. In Ar post-discharges the main sterilizing agents are believed to be the VUV photons (105-107 nm) emitted by the Ar atoms in the resonant states, whereas in Ar-O₂ mixture the VUV photons and O atoms. In the Ar-O₂ system N₂ molecules can be also present as impurities, which makes possible the formation of UV emitting excited NO molecules. The enhanced UV emission in the Ar-O₂-N₂ can increase the sterilization efficiency of the system. As a matter of fact, the inactivation effectiveness of the Ar-O₂-N₂ ternary mixture has been recently investigated in a low pressure ICP discharge by Kylián et al. [3].

The aim of this work is to investigate the evolution of the densities of active species produced by flowing Ar-O₂ and Ar-O₂-N₂ microwave discharges in the discharge region and in the early-afterglow, thus contributing to the understanding of the elementary processes occurring in these systems, in particular those responsible for plasma sterilization.

2. System set-up

The investigated system is similar to the one used in the sterilization experiments by the Montréal group [4]. Here the surface wave discharge is generated with 2450 MHz field frequency in a 10 mm diameter tube. The discharge and the reactor are linked through two tubes of different diameters, whereas the first tube, right after the discharge zone, has the same diameter as the discharge tube, the second tube is widened to 2.6 cm relatively to the discharge tube and it enters in the post-discharge reactor in the middle of the west plane. The inlet and outlet are sym-

metrically positioned on the west and bottom walls, respectively, so that only one half of the chamber needs to be considered for the simulation. The discharge tube is made of fused silica, while the reactor is of aluminium.

Herein we focus our attention on the discharge and early afterglow region. We assume that the radius of the tube where the early-afterglow develops has the same size as the discharge tube. The calculations are conducted for surface wave discharges generated in Ar-O₂ and Ar-O₂-N₂ mixtures at p=2 Torr, which is typical operation condition in the sterilization experiments [4,5].

3. Model

The discharge and early afterglow regions of the system are described with a kinetic model. The species densities in the discharge region are calculated by solving the homogeneous electron Boltzmann equation, coupled together with the rate balance equations of the different heavy-particles. The concentrations obtained for the steady-state discharge are used as initial values to the early afterglow taking place in the tube connecting the discharge to the main reactor, where the same system of equations is solved in time under zero electric field [6].

As discussed in the previous section, in actual sterilization devices the active species subsequently enter a large volume reactor where the late-afterglow develops. The modelling of the complete system will be pursued in the near future, by following the evolution of the species densities in the post-discharge reactor with a 3-D hydrodynamic model [5].

In the model of the Ar-O₂ system the species taken into account are: Ar(¹S₀, ³P₂, ³P₁, ³P₀, ¹P₁), O₂(X³Σ_g⁻, v), O₂(a¹Δ_g, b¹Σ_g⁺), O(³P, ¹D), O₃, Ar⁺, Ar₂⁺, O₂⁺, O⁺, O⁻; while in the Ar-N₂-O₂ system the N containing species are still added, i.e.: N₂(X, v), N(⁴S, ²D, ²P), N₂(A, B, B', C, a', a, w), NO₂(X, A), NO(X, A, B), N₂⁺(X, B), N₄⁺ and NO⁺. The set

of gas phase reactions describing the kinetics of species as considered in the post-discharge chamber and discharge region for the nitrogen and oxygen containing species has been presented in [6,7] and the references therein. A set of reactions for the Ar, Ar-N₂ and Ar-O₂ mixtures can be found in [8-10]. The surface reactions involving the N and O atoms have been discussed in details in [5].

4. Results

From the applications point of view the important species in the discharge and afterglow are the active atoms as: ground state N(⁴S) and O(³P) atoms, and excited O(¹D); metastable atoms Ar(³P₀, ³P₂); UV/VUV emitting atoms and molecules such as Ar(¹P₁, ³P₁), NO(A), NO(B).

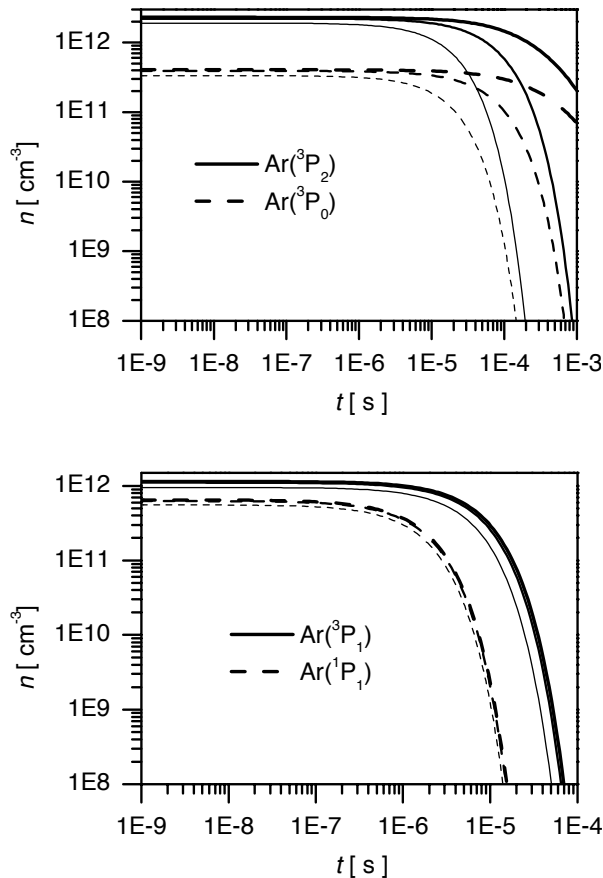


Figure 1. The evolution of the metastable and resonant state Ar atoms density along the early afterglow ($t=0$ means the end of the discharge) in Ar (thick line) and in Ar-O₂ mixture with 0.2% and 1%O₂ addition (thin line).

As a first step the density of species created in pure Ar and Ar-O₂ discharges have been calculated and further the evolution of their densities in the early-afterglow as a function of afterglow time (which is correlated to the length of the afterglow tube through the gas flow) have been followed.

Figure 1 shows the time evolution of the Ar(4s) states in the early afterglow in case of Ar discharge and of an Ar-O₂ discharge with different oxygen addition. It is clearly seen that the metastable states Ar(³P₀, ³P₂) are strongly quenched upon O₂ addition in the mixture. This is a result of the very efficient destruction by reactions $\text{Ar}(\text{}^3\text{P}_0, \text{}^3\text{P}_2) + \text{O}_2 \rightarrow \text{Ar}(\text{}^1\text{S}_0) + \text{O}(\text{}^3\text{P}) + \text{O}(\text{}^3\text{P}, \text{}^1\text{D})$. For O₂ percentages as low as 1%, these metastable states do not survive for afterglow times larger than 10⁻⁴ s.

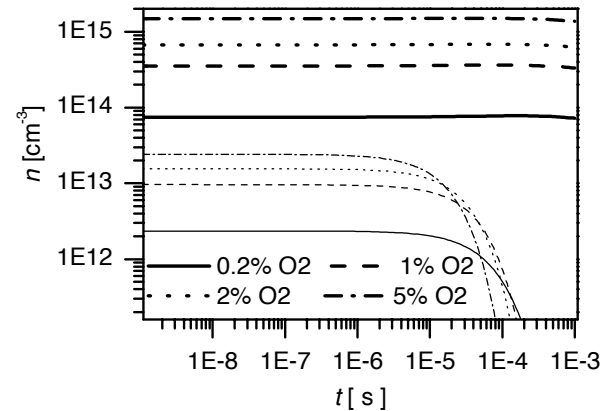


Figure 2. The evolution of O(³P) (thick lines) and O(¹D) (thin lines) atoms density along the early afterglow in Ar-O₂ mixture with different O₂ addition.

The evolution of oxygen O(³P) and O(¹D) atoms is depicted in Figure 2. Ground-state O(³P) atoms (thick lines) remain approximately constant in the afterglow, whereas O(¹D) is quenched much faster, mostly in collisions with Ar atoms, at the wall, with O₂ (in a process forming O₂(b)) and with O(³P). On the other hand, the density of oxygen atoms rises steeply upon oxygen addition into an argon discharge, as it would be expected. Notice that oxygen is strongly dissociated by electron impact and by the Ar metastables, the dissociation degree being in the range of 25-50%. Similar results have also been obtained experimentally by Mozetič et al. [11] where the density of O(³P) ground state atoms have been determined both by NO titration and catalytic probe methods.

In the next step we have investigated the evolution of the densities of Ar and oxygen containing species with the addition of N₂ to the Ar-2%O₂ mixture. Further, the creation of the nitrogen containing species such as the UV emitting excited NO(A) and NO(B) molecules have been followed.

The concentration of O(³P) and O(¹D) atoms is plotted in Figure 3 for Ar-O₂-N₂ mixtures containing 2%O₂ and nitrogen admixture in the range of 0-2%, whereas Figure 4 illustrates the evolution of N(⁴S), NO(A) and NO(B) for the same conditions. The small increase in the O(³P) concentration revealed by Figure 3 corresponds to the nearly total conversion of O(¹D) into O(³P). In case of O(³P) it can also be observed that its density do not change monotonically.

cally with the N_2 addition, it decrease up to the 0.1% N_2 addition and then it increases again above the value obtained in no nitrogen containing Ar- O_2 mixture. In turn, Figure 4 shows that the populations of nitrogen-containing species rise monotonically with N_2 addition. NO(A) is mainly formed by the reaction $N_2(A)+NO(X) \rightarrow N_2(X,v=0)+NO(A)$ and lost by radiative decay. On the other hand, NO(B) is formed by 3-body reassociation $N+O+M \rightarrow NO(B)+M$, with $M=Ar$ (predominantly), N_2 and O_2 . Similarly to the case of NO(A), its losses are essentially a consequence of its radiative decay.

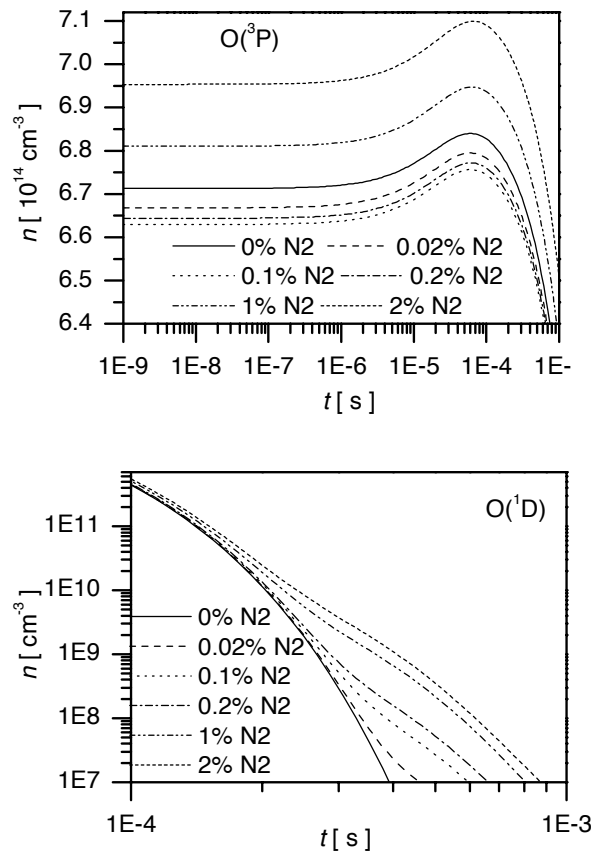


Figure 3. The evolution of $O(^3P)$ and $O(^1D)$ atoms density along the early afterglow in Ar- O_2 - N_2 mixture different $N_2\%$ addition to Ar-2% O_2 .

The present investigation confirms that the ternary mixture Ar- O_2 - N_2 leads to an efficient production of active species in the limit of relatively low concentrations of O_2 and N_2 . The production of active species relevant for sterilization processes requires a relatively short early-afterglow, preferably below 10^{-4} s. Different tube radii and wall material may contribute to optimize the process, mostly by increasing the characteristic times for the wall losses of oxygen atoms.

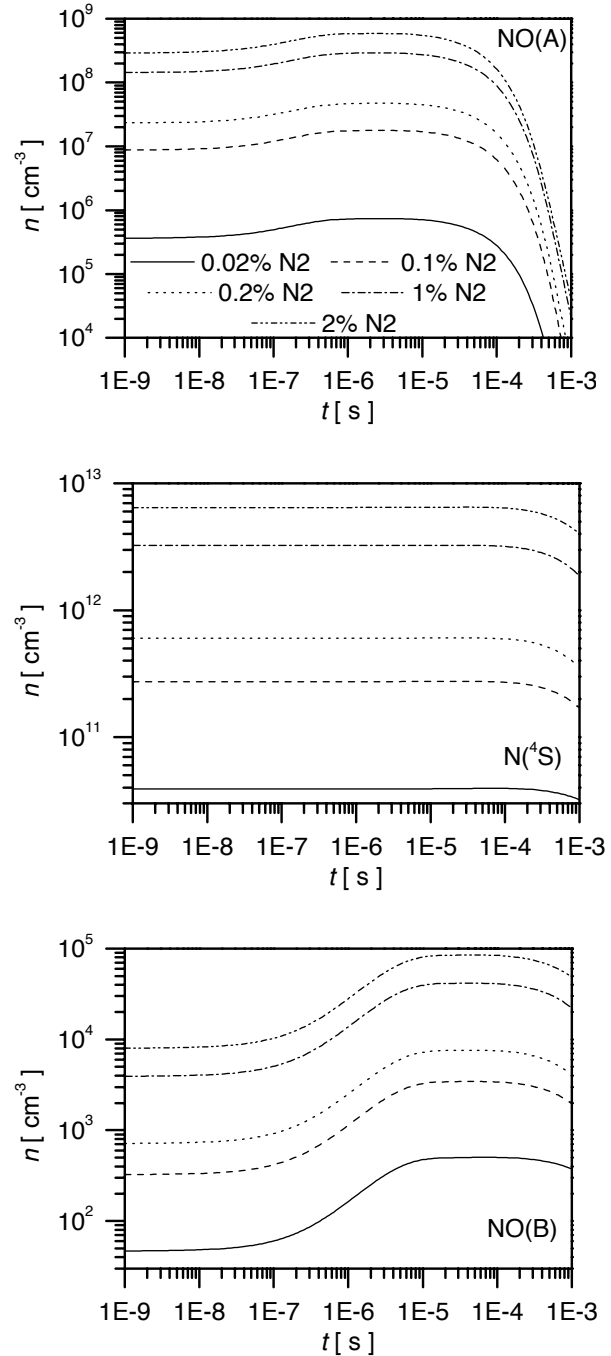


Figure 4. The density of NO(A), $N(^4S)$ and NO(B) as a function of the early afterglow time in case of an Ar- O_2 - N_2 discharge, when the O_2 percentage is set to 2% and the N_2 addition varies in the 0-2% range.

Acknowledgement

The work has been supported by the Hungarian Science Foundation OTKA, through project F-67556, Bolyai Fellowship of K.K. and Portuguese Science Foundation FCT.

References

- [1] T. Belmonte et al., Surf. Coat. Technol., **97**, 642 (1997).
- [2] S. Moreau, M. Moisan, M. Tabrizian, J. Barbeau J. Peltier, A. Ricard, J. Appl. Phys., **88**, 1166 (2000).
- [3] O. Kylián and F. Rossi, J. Phys. D: Appl. Phys., **42**, 085207 (2009).
- [4] K. Kutasi, B. Saoudi, C. D. Pintassilgo, J. Loureiro, M. Moisan, Plasma Processes and Polymers, **5**, 840 (2008).
- [5] K. Kutasi and J. Loureiro, J. Phys. D: Appl. Phys., **40**, 5612 (2007).
- [6] C. D. Pintassilgo, J. Loureiro, V. Guerra J. Phys. D: Appl. Phys., **38**, 417 (2005)
- [7] K. Kutasi, C. D. Pintassilgo, J. Loureiro, P. J. Coelho, J. Phys. D: Appl. Phys., **40**, 1990 (2007).
- [8] C. M. Ferreira, J. Loureiro, A. Ricard, J. Appl. Phys., **57**, 82 (1985).
- [9] J. T. Gudmundsson and E. G. Thorsteinsson, Plasma Sources Sci. Technol. **16**, 399 (2007); T. Sato and T. Makabe J. Phys. D: Appl. Phys. **41** 035211 (2008).
- [10] P. Sá and J. Loureiro, J. Phys. D: Appl. Phys., **30**, 2320 (1997).
- [11] M. Mozetič et al., J. Vac. Sci. Technol. A **21**, 369 (2003)